Johnson, W. J., Bamberger, M. J., Latta, R. A., Rapp, P. E., Phillips, M. C., & Rothblat, G. H. (1986) *J. Biol. Chem. 261*, 5766-5776.
Johnson, W. J., Mahlberg, F. H., Chacko, G. K., Phillips, M. C., & Rothblat, G. H. (1988) *J. Biol. Chem. 263*, 14099-14106.
Karlin, J. B., Johnson, W. J., Benedict, C. R., Chacko, G. K., Phillips, M. C., & Rothblat, G. H. (1987) *J. Biol. Chem. 262*, 12557-12564.
Lange, Y., Culter, H. B., & Steck, T. L. (1980) *J. Biol. Chem. 255*, 9331-9336.
Mendel, C. M., & Kunitake, S. T. (1988) *J. Lipid Res. 29*, 1171-1178.
Mendez, A. J., Oram, J. F., & Bierman, E. L. (1991) *J. Biol. Chem. 266*, 10104-10111.
Milner, T. G., Ko, K. W. S., Ohnishi, T., & Yokoyama, S. (1991) *Biochim. Biophys. Acta 1082*, 71-78.
Nishikawa, O., Yokoyama, S., Kurasawa, T., & Yamamoto, A. (1985) *J. Biochem. 99*, 295-301.
Okabe, H., Yokoyama, S., & Yamamoto, A. (1988) *J. Biochem. 104*, 141-148.
Oram, J. F., Brinton, E. A., & Bierman, E. L. (1983) *J. Clin. Invest. 72*, 1611-1621.
Rothblat, G. H., & Phillips, M. C. (1982) *J. Biol. Chem. 257*, 4775-4782.
Slotte, J. P., Oram, J. F., & Bierman, E. L. (1987) *J. Biol. Chem. 262*, 12904-12907.
Stein, O., & Stein, Y. (1973) *Biochim. Biophys. Acta 326*, 232-244.
Tabas, I., & Tall, A. R. (1988) *J. Biol. Chem. 259*, 13897-13905.
Tajima, S., Yokoyama, S., & Yamamoto, A. (1983) *J. Biol. Chem. 258*, 10073-10082.
Tajima, S., Yokoyama, S., & Yamamoto, A. (1984) *J. Biochem. 96*, 1753-1767.
Werb, Z., & Cohn, Z. A. (1971) *J. Exp. Med. 134*, 1545-1590.
Yeagle, P. L. (1985) *Biochim. Biophys. Acta 822*, 267-287.
Yeagle, P. L., & Young, J. E. (1986) *J. Biol. Chem. 261*, 8175-8181.
Yokoyama, S. (1990) *Biochim. Biophys. Acta 1047*, 99-101.
Yokoyama, S., Tajima, S., & Yamamoto, A. (1982) *J. Biochem. 91*, 1267-1272.
Yokoyama, S., Kawai, Y., Tajima, S., & Yamamoto, A. (1985) *J. Biol. Chem. 260*, 16375-16382.

Association and Metabolism of Exogenously-Derived Lysophosphatidylcholine by Cultured Mammalian Cells: Kinetics and Mechanisms

Jeffrey M. Besterman[‡] and Paul L. Domanico*[,§]
Departments of Cell Biology and Biochemistry, Glaxo Research Institute, Glaxo Inc., Research Triangle Park, North Carolina 27709
Received March 22, 1991; Revised Manuscript Received October 8, 1991

ABSTRACT: The association and metabolism of exogenously-derived lysophosphatidylcholine (lysoPC) with cultured mammalian cells from a variety of sources was studied, and a mechanism was defined by computer modeling for Vero cells. Cell monolayers were incubated with radiolabeled lysoPC, and the kinetics of disappearance from the medium, association with the cells, and metabolism by the cells of lysoPC were monitored both in the absence and in the presence of fetal bovine serum. Exogenously-supplied lysoPC first associated with cell membranes, followed by an almost complete conversion to phosphatidylcholine (PC). The kinetics of partitioning and metabolism were identical regardless of whether the exogenously-supplied lysoPC was labeled with [*methyl*-^{3}H]choline or with [1-^{14}C]palmitate. A two-step mechanism, consisting of a reversible partitioning of exogenous lysoPC into the cell membrane followed by enzymatic reacylation to PC, was found to adequately describe the observed kinetics in the presence of 0 or 0.5% fetal bovine serum. The effect of temperature on the individual rate constants and on the overall process was examined. An Arrhenius plot indicated an acute temperature sensitivity between 15 and 23 °C, consistent with a dependence on the lipid phase of the membrane and a regional phase transition temperature characteristic of mammalian cells. The acute temperature sensitivity was almost entirely due to the temperature dependence of reacylation. A multistep mechanism was established by combining the kinetic constants determined under conditions of low exogenous protein with the binding constant between lysoPC and serum protein. This mechanism accurately predicts the rates of uptake of exogenously-derived lysoPC with cultured cells in the presence of serum concentrations between 0 and 10%. A survey of a variety of cultured cells indicated that the kinetics of association and metabolism of exogenously-derived lysoPC is cell-type specific.

Phosphatidylcholine (PC) is the major phospholipid component of cellular membranes. It is an important substrate for hormone-activated phospholipases. Moreover, lysophosphatidylcholine (lysoPC) has been shown to be a stereospecific chemoattractant for mouse lymphoblastic cells (Hoffman et al., 1982) and for human monocytes (Quinn et al., 1988), and it has been postulated that lysoPC may be generated at sites of inflammation, tissue injury, and repair (Hoffman et al., 1982; Quinn et al., 1988). In addition, one causative agent of schistosomiasis, the parasite *Schistosoma mansoni*, uses lysoPC to lyse adherent human red blood cells

* Address correspondence to this author at the following address: Department of Biochemistry, Glaxo Research Institute, 5 Moore Drive, Research Triangle Park, NC 27709.
‡ Department of Cell Biology.
§ Department of Biochemistry.

0006-2960/92/0431-2046$03.00/0

and to fuse with human neutrophils (Golan et al., 1986). Experiments designed to study the regulation of agonist-induced cellular turnover of PC required mammalian cells labeled with exogenous lysoPC as well as a clear understanding of the mechanism of association and metabolism of exogenously-derived lysoPC. However, except for work in the area of red blood cells, very little had been done to study this phenomenon. The present study was designed to define the mechanism underlying the association and metabolism of exogenously-derived lysoPC by cultured mammalian cells from a variety of sources under both serum-free and serum-containing conditions. Vero cells were chosen as the model cell, and the experimental culture conditions were those commonly used for studying agonist-induced turnover of membrane phospholipids.

Materials and Methods

Cell Culture. Vero cells, mink lung cells (Mv 1 Lu), and Madin–Darby canine kidney cells were grown in MEM[1] supplemented with 10% FBS. HL-60 cells were grown in RPMI 1640 supplemented with 10% FBS. Primary neuronal cultures from fetal rat brain were obtained from 16-day-old rat embryos and maintained serum-free in basal medium of Eagle with Earle's salts and L-glutamate/Ham's F-12 (1:1), with glucose, glutamine, penicillin, streptomycin, transferrin, and 1 μM insulin, all as described (Burgess et al., 1986, 1987). Primary cultures of rat brain astrocytes, oligodendrocytes, and meningeal fibroblasts were prepared from 1–2-day-old pups and maintained in the neuronal medium in the presence of 10% FBS, all as described (Burgess et al., 1985, 1987).

Experimental Design. Vero cells were grown to confluence in 35-mm dishes, followed by incubation for 24–48 h in MEM, 0.5% FBS. All experiments were performed on confluent Vero cell monolayers in MEM, 0.5% FBS at pH 7.4, in a humidified atmosphere of 95% air, 5% CO_2 at 37 °C, unless indicated otherwise. Temperatures reported were maintained within a tolerance of ±1 °C. Experiments were initiated by addition of 2 μM [^{14}C]lysoPC, unless indicated otherwise. Incubation in the presence of labeled lysoPC was terminated by aspiration of medium, rapid washing of the cell monolayer five times with ice-cold MEM, 0.5% FBS, and reincubation if required. To terminate the experiment, the monolayers were extracted with chloroform/methanol (1:2 v/v). After separation of the phases, the appropriate samples were taken for analysis.

Association of lysoPC with plasma membrane was further verified as follows. Vero cells were labeled with [^{14}C]lysoPC as above. These cells were placed on ice, scraped from plates into ice-cold 25 mM Hepes, 5 mM $MgCl_2$, pH 7.3, and passed repeatedly through a 27-gauge needle. The cell homogenate was centrifuged at 600g for 10 min at 4 °C. The 600g supernatant was centrifuged at 10000g for 25 min at 4 °C. Finally, the 10000g supernatant was centrifuged at 150000g for 60 min at 4 °C. The distribution of radiolabel was measured for all supernatants and pellets, and it was found to correlate with the distribution of 5′-nucleotidase activity, an enzyme marker known to associate with plasma membrane (Avruch & Wallach, 1971). The 5′-nucleotidase activity distribution was determined by measuring the release of inorganic phosphate from 5′-AMP with the Fiske–Subbrow Assay (Kuby et al., 1954).

All data reported are the mean of three experiments, with each experiment performed in duplicate. Standard errors were less than or equal to 10% of the mean. In those studies where the FBS percentage was varied, the rest of the procedure was identical to that described above.

The raw data is measured in DPM and is converted to nanomoles of lysoPC via the specific activity of the substrate. Because the serum may contain some lysoPC, the absolute specific activity in the experiments will change. However, this does not affect the rates or rate constants since the actual specific activity is constant. Since the actual amount of lysoPC in serum is unknown, all data including graphs will be expressed in terms of the amount of [^{14}C]lysoPC added to the serum. Studies identical to those described here were performed using [^{3}H]lysoPC. Similar results were obtained (data not shown).

Preloading of Cells with lysoPC at 15 °C. For experiments requiring preloading of cells with lysoPC, monolayers were incubated with radiolabeled lysoPC for 4 h at 15 °C, after which the monolayers were washed five times with ice-cold MEM, 0.5% FBS and immediately reincubated as described.

Heat-Inactivation of Cell Monolayers. For protocols requiring heat-inactivation of the cell monolayers prior to kinetic analysis, the monolayers were manipulated as follows. The dishes containing the monolayers were incubated at 60 °C by setting the dishes on aluminum blocks for 5 min. The temperature of the aluminum blocks was maintained with a water bath. The dishes were rapidly cooled by placing them on ice, and finally the dishes were incubated at 37 °C for 30 min to allow for cellular recovery from heating. Prior to the addition of radiolabeled lysoPC, the dishes were incubated at the desired experimental temperature for 30 min. Throughout the course of the subsequent experiments involving heat-inactivated cells, all monolayers heat-inactivated in this manner remained intact and as viable as control cells. This was determined by phase contrast microscopy and the ability of the cells to exclude trypan blue after the cells were subjected to a 2-h incubation period under experimental conditions. Morphologically, however, the heat-inactivated monolayers could be distinguished from control monolayers by a slightly altered structure, increased refractoriness of the cytoplasm, and the time-dependent appearance of openings in the monolayer.

Thin-Layer Chromatography. Radiolabeled species were separated using silica gel 60A, LK6D chromatography plates (Whatman). The solvent system consisted of chloroform/methanol/1 N acetic acid (65:25:4). This system was chosen for its ability to separate lysoPC, PC, and free fatty acids. Carrier consisting of 70 μg of PC, 70 μg of lysoPC, 140 μg of phosphatidate, and 140 μg of oleic acid was added to all samples to permit visualization by iodine vapor. Spots were scraped from the plates, placed in scintillation vials, and counted as an emulsion using 2 mL of water and 4 mL of Scintiverse II (Fisher).

Determination of the lysoPC·Serum Protein Binding Constant. The apparent disassociation constants between ^{14}C-labeled lysoPC and fatty acid-free BSA or protein(s) in FBS were determined by gel retardation analysis. A 200-μL solution containing 10 μM lysoPC (0.2 μCi/mL) and 0 to 10% FBS in MEM was preincubated at 37 °C for 4 h. A 130-μL aliquot of the above mixture was gently mixed with 10 μL of a 50% glycerol, 0.1% bromophenol blue solution. Each sample was loaded in duplicate at 30 μL per lane onto a native, 10% polyacrylamide gel (1.5 mm, 8 cm × 10 cm) that had been preelectrophoresed to equilibrium with a circulating MEM buffer system. Electrophoresis was performed for 1 h at 75 mA and 25 °C with the circulating MEM buffer system. The gels were vacuum dried on 3MM Whatman paper, and the

[1] Abbreviations: BSA, bovine serum albumin; MEM, minimal essential medium; lysoPC, lysophosphatidylcholine; PC, phosphatidylcholine; FBS, fetal bovine serum; RPMI, Roswell Park Memorial Institute.

[^{14}C]lysoPC protein complexes were visualized by autoradiography. The labeled band was excised, minced, and added to a vial containing an emulsion of Scintiverse II (Fisher) and water. The samples were then analyzed with an LKB liquid scintillation counter.

To compensate for the potential error arising from the quenching of the ^{14}C label by polyacrylamide, the ^{14}C counting efficiency under these experimental conditions was determined in duplicate. Thirty-microliter aliquots from the above binding study were added to 75 μL of a 10% polyacrylamide solution. After the solution polymerized, the gel pellets were vacuum dried on 3MM Whatman paper, minced, and then added to vials containing an emulsion of Scintiverse II and water. The samples were then analyzed with an LKB liquid scintillation counter.

Due to the positive charge on the lysoPC, only the [^{14}C]-lysoPC bound to either BSA or the proteins in FBS will migrate into the native polyacrylamide gel. The amount of [^{14}C]lysoPC was held constant to avoid overexposure of the autoradiogram, and the FBS concentration was varied from 0 to 10%. All concentrations of FBS were performed in duplicate.

A binding study for fatty acid-free BSA was performed, in duplicate, at concentrations that mimicked the amount of BSA in the FBS samples. It is significant to note that, regardless of the protein source, FBS, or fatty acid-free BSA, only one radiolabeled band was observed per lane and these bands comigrated. This strongly suggests that the major if not only protein interacting with lysoPC in FBS is BSA.

The simple dissociation equation

$$K_d = \frac{[\text{lysoPC}]_{\text{free}}[\text{BSA}]_{\text{free}}}{[\text{complex}]_{\text{total}}}$$

was modified to incorporate total lysoPC where $[\text{lysoPC}]_t = [\text{lysoPC}]_f + [\text{complex}]_t$ and total BSA where $[\text{BSA}]_t = [\text{BSA}]_f + [\text{complex}]_t$. This yields the binomial equation

$$[\text{complex}] = \frac{-b - \sqrt{b^2 - 4c}}{2}$$

where $b = [\text{lysoPC}]_t + [\text{BSA}]_t + K_d$ and $c = [\text{lysoPC}]_t[\text{BSA}]_t$. Using gel shift analysis and the above equation, a K_d of 5 ± 1 μM was determined for both FBS and BSA. This is an apparent dissociation constant since no attempt was made to determine the number of lysoPC molecules bound per molecule of BSA.

Computer Modeling. NONLIN84 version V02 is a VAX-based software product from Statistical Consultants, Inc. This software uses a mathematical nonlinear model, created by the user, and a data set to estimate the rate constants. The proposed mechanistic scheme is translated into a series of differential equations that define the relationships between the various chemical species. The rate constants are constrained a priori to realistic boundaries; for example, all the values must be greater than or equal to zero. A "best fit" of the rate constants is achieved by a modified version of the Gauss–Newton algorithm (Hartley, 1961). The results of this iteration are rate constants and their statistical significance. The error in a rate constant is a function of the ratio of the number of differential equations to the number of data points.

Materials. The following reagents were obtained from the indicated sources: 1-[1-^{14}C]palmitoyl-L-lyso-3-phosphatidylcholine, 58.5 mCi/mmol (Amersham); L-α-dipalmitoyl-[*choline methyl*-^{3}H]phosphatidylcholine, 51 Ci/mmol (New England Nuclear); oleic acid, L-α-phosphatidic acid (dioleoyl), 1-palmitoyl-*sn*-glycerophosphocholine, dipalmitoyl-lysoPC, and porcine pancreas phospholipase A_2 (Sigma).

1-Palmitoyl-*sn*-glycerophospho[*methyl*-^{3}H]choline was prepared from L-α-dipalmitoyl[*choline methyl*-^{3}H]phosphatidylcholine by the hydrolytic action of phospholipase A_2.

Results

Kinetics of Association and Metabolism of Exogenously-Derived lysoPC with Vero Cells. To determine the kinetics of lysoPC association with and metabolism by Vero cells, monolayers of Vero cells were incubated with 2 μM [^{14}C]lysoPC at 37 °C, and the radioactive content of both the medium and the cells was measured. Figure 1 (symbols) shows the time course for the disappearance of lysoPC from the media, its association to the membrane, and subsequent conversion to PC via reacylation. Identical studies were performed using 1-palmitoyl-*sn*-glycerophospho[*methyl*-^{3}H]choline, and similar results were obtained (data not shown). This suggests that under our conditions lysoPC is not degraded.

To elucidate the mechanism underlying the observed kinetics of association and metabolism of lysoPC by Vero cells, data was analyzed with the iterative, nonlinear computer software package NONLIN84. The data was fit to a simple two step process where each step is first order (mechanism 1). However, the best fit curves derived from mechanism 1 (data not shown) either overestimated or underestimated the data in a statistically systematic fashion. The difference between the observed and predicted values appeared to be due to an unsatisfactory description of the first step (association) because the cellular uptake of lysoPC was not first order.

mechanism 1

$$\text{lysoPC}_{\text{media}} \rightarrow \text{lysoPC}_{\text{membrane}} \rightarrow \text{PC}_{\text{membrane}}$$

An accurate model of the experimental kinetics was achieved by modifying mechanism 1 to included a reversible association step (mechanism 2) where k_1 = the association of lysoPC with the membrane, k_2 = the dissociation of lysoPC from the membrane, and k_3 = the acylation of lysoPC to PC. The kinetics of lysoPC association and metabolism by Vero cells were described quite well by mechanism 2 (Figure 1, lines) and yielded the following rate constants: $k_1 = 0.056 \pm 0.012$ min^{-1}, $k_2 = 0.089 \pm 0.029$ min^{-1}, and $k_3 = 0.023 \pm 0.002$ min^{-1}.

mechanism 2

$$\text{lysoPC}_{\text{media}} \underset{k_2}{\overset{k_1}{\rightleftharpoons}} \text{lysoPC}_{\text{membrane}} \xrightarrow{k_3} \text{PC}_{\text{membrane}}$$

To confirm that the membrane-associated lysoPC could indeed partition between membrane dissociation and enzymatic acylation as required by mechanism 2, the following experiment was performed. Cells were preloaded with [^{14}C]lysoPC by incubation in the presence of 2 μM [^{14}C]lysoPC for 4 h at 15 °C, at which time approximately 0.77 nmol of the [^{14}C]lysoPC was membrane-associated. Of that, 0.30 nmol (40%) of the cell-associated radiolabel was lysoPC and 0.47 nmol (60%) was PC. After the monolayers were washed at 4 °C, the cells were reincubated with isotope-free medium at 37 °C, and the egress of radiolabel into the medium was monitored and characterized. Figure 2 shows the disassociation of membrane-bound lysoPC into the media with time. The data indicate that the cell-associated [^{14}C]lysoPC dissociated from the cellular membrane and reached a maximum amount after 15 min, as predicted by mechanism 2. Furthermore, over 95% of the label reappearing in the medium was lysoPC. This indicates that membrane PC did not dissociate into the medium. Thus, mechanism 2 represents a

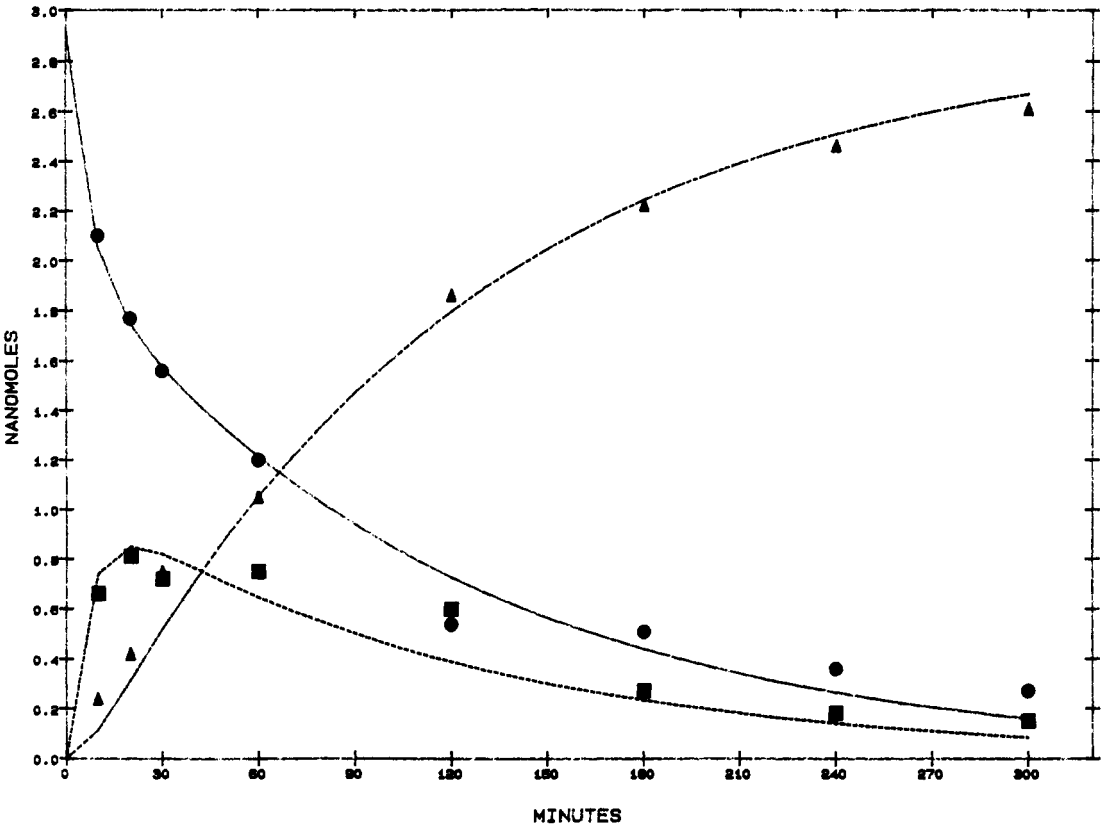

FIGURE 1: Distribution of [^{14}C]lysoPC and metabolites following incubation with cultured Vero cells at 37 °C. The symbols indicate the distribution of radiolabel where the filled circles indicate the medium [^{14}C]lysoPC, the filled squares indicate cell membrane [^{14}C]lysoPC, and the filled triangles indicate cell membrane [^{14}C]PC. The curves are the best fit to mechanism 2, where the solid curve represents the medium lysoPC data, the dashed curve represents the membrane lysoPC data, and the dot-dot-dashed curve represents the membrane PC data. See text for further details. The acylation of lysoPC to PC, k_3, should be viewed as the flux through this step and, therefore, includes the phospholipase A_2-catalyzed hydrolysis of PC to lysoPC. However, the amount of PC hydrolysis is insignificant when compared to the amount of lysoPC acylation where at 5 h nearly all of the membrane-bound lysoPC is converted to PC. Throughout the course of the experiment, between 93% (at 10 min) and 99% (at 300 min) of the cell-associated, radiolabeled lysoPC was cell-membrane associated as demonstrated by analysis of the organic phase of the cell extract. The association of the lysoPC with the cell membrane was further verified by cell fractionation and differential centrifugation. In this series of experiments, over 95% of all the cell-associated radiolabeled lysoPC was shown to be membrane associated as demonstrated by an identical pellet distribution to that of plasma membrane-associated 5′-nucleotidase (Avruch & Wallach, 1971).

simple and adequate description of the partitioning and metabolism of exogenously-derived lysoPC by Vero cells and indicates that k_1, k_2, and k_3 are of the same magnitude, with k_3 as the slowest and, therefore, the rate-limiting step.

Effects of Temperature on the Kinetics of Partitioning and Metabolism of Exogenously-Derived lysoPC by Vero Cells. Often, membrane-associated processes show a dependence on the lipid phase of the bilayer which results in a pronounced temperature dependence (Chapman, 1975; Melchior & Stein, 1976; Rule et al., 1980; Ryan & Simoni, 1980; Burns & Dudley, 1982). The association with and the metabolism of lysoPC by Vero cells is no exception. Cells were incubated with [1-^{14}C]lysoPC at temperatures between 15 and 37 °C, and the disappearance of lysoPC from the medium was measured. The rates of disappearance yield half-lives that ranged from approximately 1 h at 37 °C to approximately 11 h at 15 °C. The overall half-life is defined as that time at which half of the lysoPC in the media has been taken up by the cells. When these half-lives were depicted as an Arrhenius plot (Figure 3), a sharp break in the slope is observed at approximately 21 °C. This sharp break is characteristic of membrane-associated processes, and a lipid phase transition temperature of 20–24 °C is characteristic of mammalian cells (Rule et al., 1980; Ryan & Simoni, 1980; Burns & Dudley, 1982).

To determine which step or steps in the pathway described by mechanism 2 were responsible for the temperature-associated break, we examined the kinetics of association and metabolism of exogenously-derived lysoPC by Vero cells as a function of temperature (15, 23.5, and 37 °C). Both experiments at 15 and 23.5 °C were fit perfectly by mechanism 2 (data not shown), which further verifies this model. The derived rate constants from these experiments are summarized in Table I.

Table I: Temperature Dependency of the Individual Rate Constants[a]

temperature		rate constants		
°C	1/K (×10^3)	k_1	k_2	k_3
15.0	3.472	0.0073	0.0464	0.0039
23.5	3.373	0.0127	0.0650	0.0196
37.0	3.226	0.0560	0.0889	0.0234

[a] The rate constant units are min^{-1}. The uncertainties of the rate constants were 25%, 25%, and 10% for k_1, k_2, and k_3, respectively.

To determine the relationship between the temperature sensitivity of each rate constant and the temperature sensitivity of the overall process, the fractional change was calculated. The fractional change is the relative change in the value of a parameter as the incubation temperature is lowered from 37 °C. To compare half-lives to rate constants, which are inversely related, the reciprocal of the half-lives and their subsequent fractional changes were determined.

An Arrhenius plot that compares the fractional change in the overall half-life to the fractional changes in k_1 and k_2 (Figure 4A) shows that there is a break for k_1 that does not

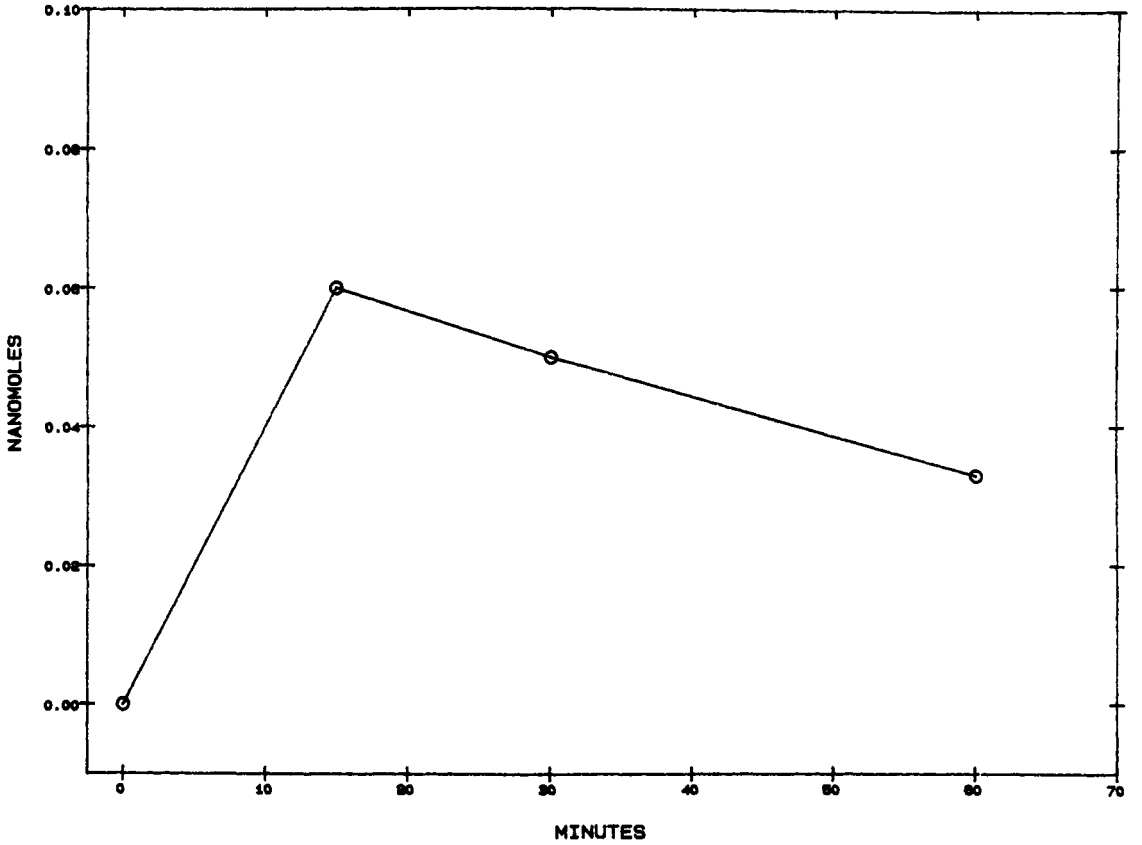

FIGURE 2: Analysis of cell-associated lysoPC released into the media. The circles indicate the [^{14}C]lysoPC in the media. The circles are connected to aid the eye. See text for futher details.

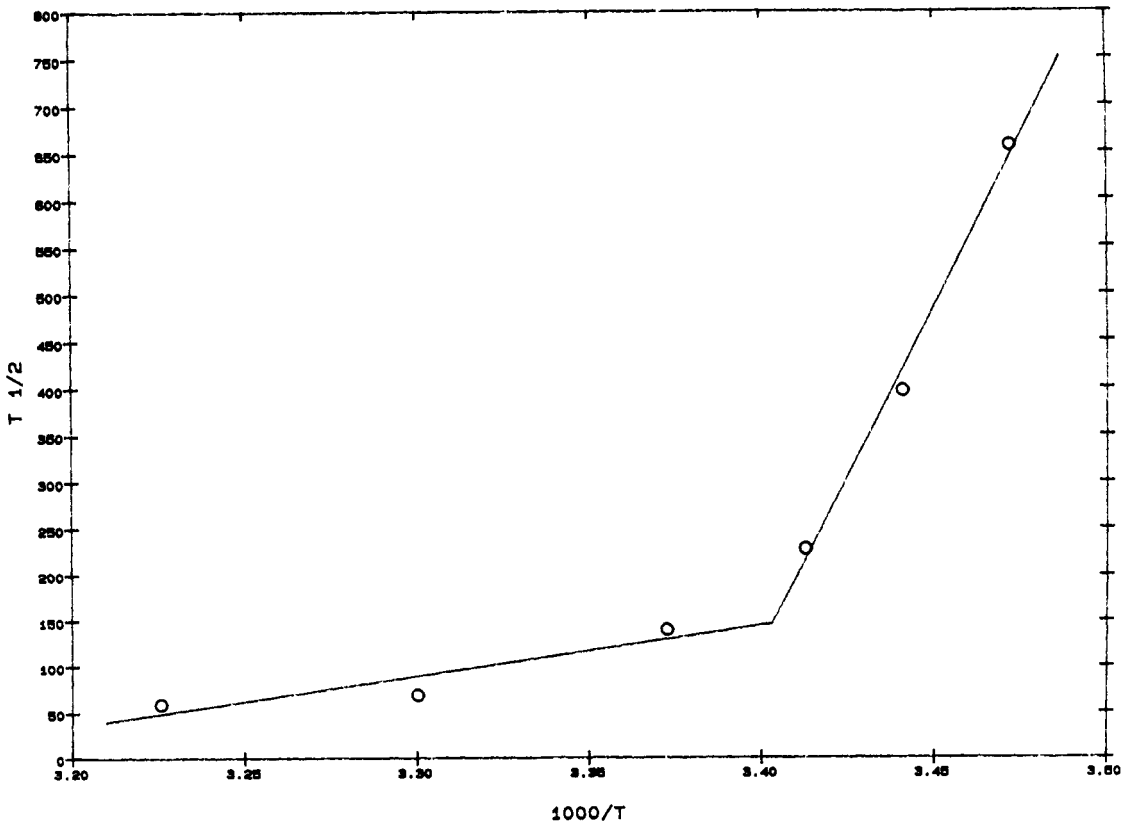

FIGURE 3: Arrhenius plot of the temperature dependence of the overall half-live determined from the metabolism of lysoPC. The overall half-lives, shown as open circles, were determined by calculating from the best fit curves the time point at which half of the lysoPC from the media had been taken up by the cells. These overall half-lives were then plotted versus 1000 times the reciprocal of the experimental temperature as given in Kelvin. The data fell into two groups—one above and one below approximately 21 °C. The curves were generated from least-squares analysis of the two groups of data. The intersection of the two least-squares curves is at approximately 21 °C. The slope of the curve below 21 °C is 10-fold greater than the slope of the curve above 21 °C. See text for further details.

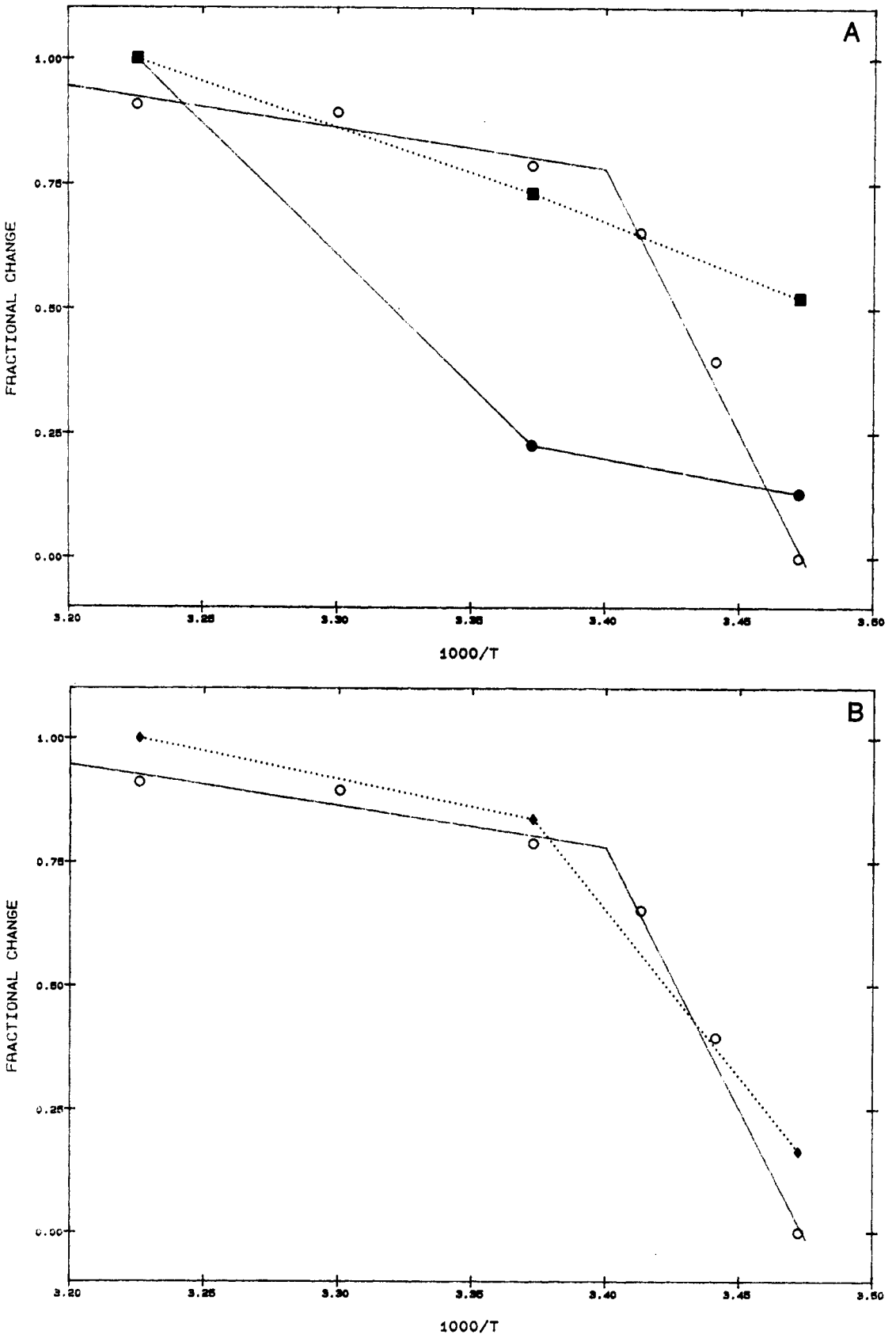

FIGURE 4: (A) Arrhenius plot comparing the fractional change in the overall half-life to the fractional changes in the rate constants k_1 and k_2. The open circles indicate 1 minus the fractional change in overall half-life as defined in the text. This was done to simplify the graphical interpretation. The filled circles and filled squares indicate the fractional changes in k_1 and k_2, respectively. The data are plotted versus 1000 times the reciprocal of the experimental temperature as given in Kelvin. The least-squares curves for the fractional change in overall half-life were generated as in Figure 3. The data from the fractional changes in k_1 and k_2 were connected with solid and dotted lines, respectively, for ease of visual representation. (B) Arrhenius plot comparing the fractional change in the overall half-life to the fractional changes in the individual rate constant k_3. The fractional change in overall half-live is represented as in (A). The filled diamonds indicate the fractional change in k_3. The data are plotted versus 1000 times the reciprocal of the experimental temperature as given in Kelvin. The data from the fractional change in k_3 was connected with a dotted line for ease of visual representation.

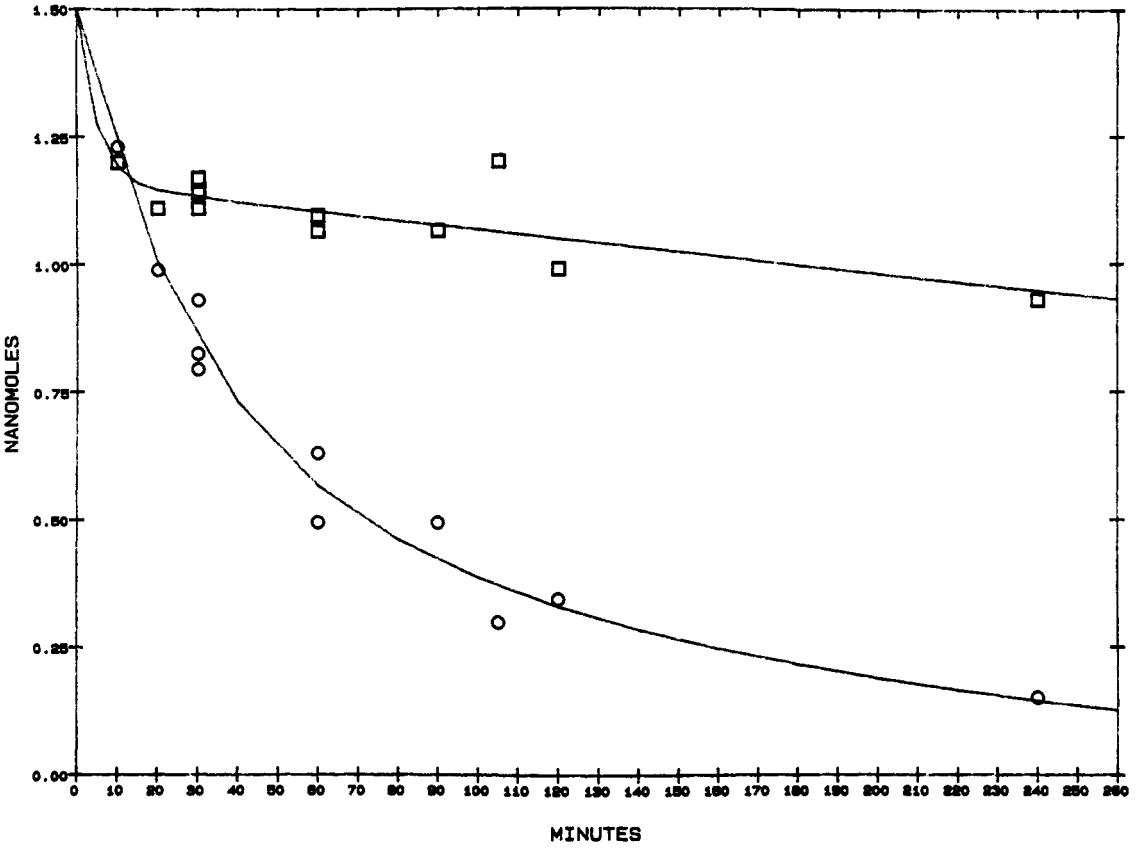

FIGURE 5: Effect of preheating cells to 60 °C for 5 min on the metabolism at 37 °C of [^{14}C]lysoPC. The symbols indicate [^{14}C]lysoPC in the media where the circles indicate [^{14}C]lysoPC in the presence of non-heat-inactivated cells and the squares indicate [^{14}C]lysoPC in the presence of heat-inactivated cells. For both the control and the heat-inactivated cells, the solid lines indicate the best fit curves to the $lysoPC_{media}$ data. See text for further details.

correspond to the break observed for the overall half-life and that k_2 is linear. Therefore, neither the profile of k_1 nor that of k_2 mimics that of the overall half-life.

However, an Arrhenius plot that compares the fractional change in the overall half-life to the fractional change in k_3 (Figure 4B) shows that there is a dramatic break in the fractional change in k_3 as a function of temperature and, furthermore, that the temperature profile of k_3 completely mimics that of the overall half-life. In conclusion, k_3 is most responsible for the break seen in the overall metabolism of lysoPC.

Isolating and Measuring the Individual Steps. The overall process of cell association of exogenous lysoPC, as described by mechanism 2, is a two-step process, consisting of partitioning into the plasmalemma (step 1 via k_1 and k_2) followed by enzymatic reacylation to PC (step 2 via k_3). To further verify this two-step model, we attempted to experimentally isolate and measure each of the mechanistic steps and to test whether the model would predict the results obtained in the following experiments.

To measure partitioning (step 1) in the absence of metabolic conversion to PC (step 2) in intact Vero cell monolayers, we attempted to heat-inactivate reacylation (step 2) and then monitor the decay of lysoPC from the medium. Although preheating the monolayer at 50 °C for 5 min had no effect (data not shown), preheating the cell monolayer at 60 °C for 5 min had a dramatic effect (Figure 5). After approximately 30 min, the amount of lysoPC in the medium reached an equilibrium, as would be predicted by mechanism 2 if k_3 equaled zero. Moreover, in control cells after 30 min, 95% of the cell-associated radiolabel was PC and 4% was lysoPC (and 1% FFA), but in preheated cells after 30 min, only 7% of the cell-associated radiolabel was PC and 65% remained as lysoPC (and 27% FFA). Thus, the heat-inactivation of the reacylation step appears nearly complete, and the ability to kinetically separate the two steps of mechanism 2 further verifies this mechanism.

To determine the temperature dependence of partitioning, cells were incubated with [^{14}C]lysoPC at various temperatures after first being heat-inactivated at 60 °C for 5 min. The rate of equilibration appeared to be almost independent of temperature. This data was fit to mechanism 2 to determine whether heat-inactivation at 60 °C was a clean paradigm for measuring step 1 in the absence of step 2 (Figure 6). The derived values for k_3 were zero at both 15 and 23 °C, and it was 0.1% of its value in non-heat-inactivated cells at 37 °C. In contrast to the non-heat-inactivated cells, however, the derived values for k_1 and k_2 were now temperature independent, as depicted by the nearly overlapping curves in Figure 6. Thus, heat inactivation successfully eliminated k_3 but in doing so altered the temperature sensitivity of k_1 and k_2.

To isolate step 2 in mechanism 2, k_2 must be much slower than k_3. After evaluation of the kinetic parameters determined above, it became apparent that it is impossible to isolate step 2 (k_3), as k_2 is larger than k_3.

Effect of Serum Concentration on the Kinetics and Mechanism of Association of Exogenously-Derived lysoPC with Vero Cells. To determine the effect of serum concentration on the kinetics and mechanism of association of exogenously-derived lysoPC with Vero cells, monolayers were incubated with 2 μM [^{14}C]lysoPC at 37 °C in the presence of 0, 0.5, 2.5, and 10% FBS, and the radioactive content of the medium was measured. The rate of uptake of exogenous lysoPC was almost identical in the presence of 0 and 0.5% FBS, but increasing

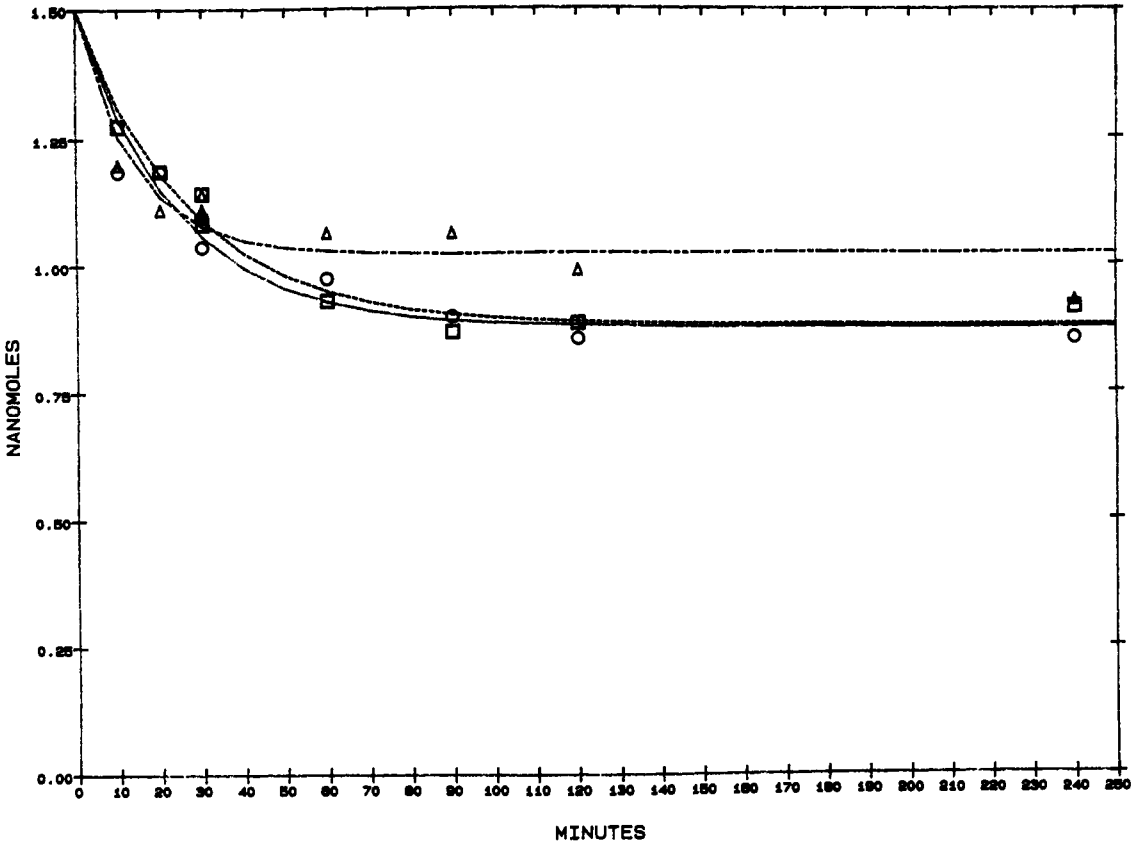

FIGURE 6: Temperature dependence of the partitioning of [^{14}C]lysoPC between medium and heat-inactivated cells. The symbols indicate [^{14}C]lysoPC in the media where the triangles indicate 37 °C, the squares indicate 23 °C, and the circles indicate 15 °C. The NONLIN84 best fit curves were generated using mechanism 2 where the dot-dot-dashed curve represents 37 °C, the dashed curve represents 23 °C, and the solid curve represents 15 °C. The plateau at the long time points represents $K_{association}$. The difference in plateau values is experimental error. See text for further details.

the concentration of FBS above 0.5% significantly retarded the rate of cellular uptake of exogenous lysoPC (Figure 7, symbols). To accurately describe the kinetics observed in the presence of 2.5 and 10% FBS, mechanism 2 required modification to include the existence of both free lysoPC and lysoPC bound to serum protein (mechanism 3) and included the following rate constants.

k_1 = the association of free lysoPC with the membrane
k_2 = the disassociation of lysoPC from the membrane
k_3 = the acylation of lysoPC to PC
k_4 = the disassociation of lysoPC from the serum BSA complex

k_5 = the association of free lyspPC with serumBSA
k_6 = the flux of lysoPC from serum-bound lysoPC to membrane-bound lyspPC

mechanism 3

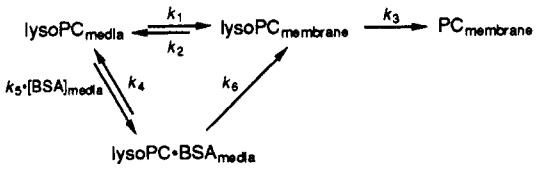

The rate constants k_1–k_6 used to describe mechanism 3 were determined as follows. The apparent K_d, k_4/k_5, for lysoPC binding to the BSA in FBS under culture conditions, was determined to be 5 ± 1 μM by gel shift analysis, as described in Materials and Methods. The data from lysoPC uptake in the absence of FBS was used to recalculate k_1, k_2, and k_3 since, in the absence of FBS, mechanism 3 degenerates to mechanism

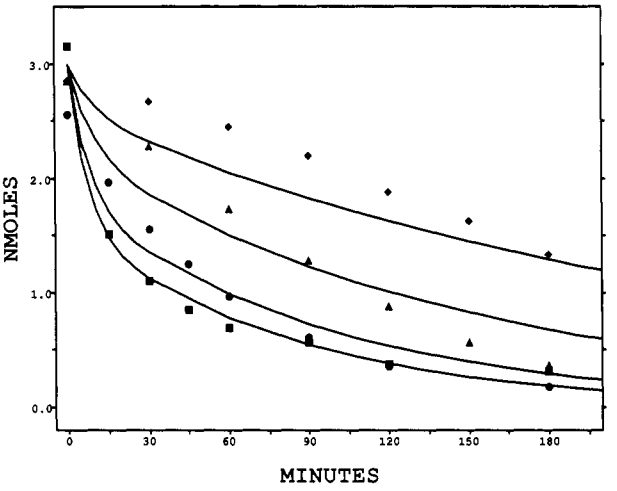

FIGURE 7: Association and metabolism of [^{14}C]lysoPC by Vero cells at 0, 0.5, 2.5, and 10% FBS. The symbols indicate [^{14}C]lysoPC in the media. The data for 0, 0.5, 2.5, and 10% FBS are indicated by squares, circles, triangles, and diamonds, respectively. The NONLIN84 best fit curves were generated using mechanism 3. See text for further details.

2. As expected, the values of k_1 and k_2 changed only slightly from 0.056 to 0.075 ± 0.020 min^{-1} for k_1 and from 0.089 to 0.069 ± 0.020 min^{-1} for k_2; however, the value of k_3 remained unchanged from its value of 0.023 ± 0.002 min^{-1} derived from mechanism 2. In conjunction with the K_d for lysoPC binding to serum protein and the rate constants k_1 and k_2, the data from lysoPC uptake in the presence of 0.5% FBS were used to determine the rate constants k_4, k_5, and k_6. (This calculation assumed that the distribution of free lysoPC to serum pro-

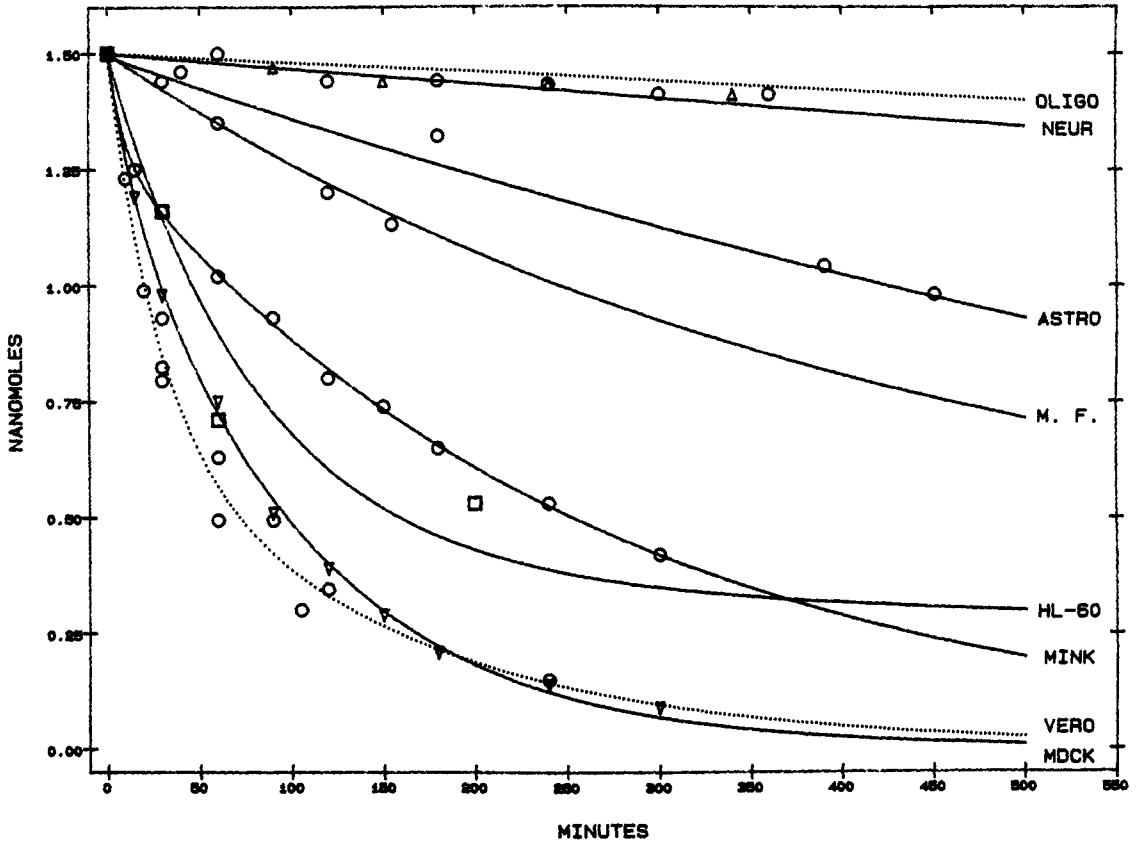

FIGURE 8: Association and metabolism of [^{14}C]lysoPC by a variety of mammalian cell types. The symbols indicate [^{14}C]lysoPC in the media. The data for astroglia (ASTRO), meningeal fibroblast (M.F.) and mink lung cells (MINK) are indicated by open circles and their curves are indicated by solid lines. The data for HL-60 cells (HL-60) is indicated by open squares and its curve is indicated by a solid line. The data for oligodendrocyte (OLIGO) and neuronal cells (NEUR) are indicated by open triangles and open circles, respectively, and their curves are shown by dotted and solid lines, respectively. The data for Madin–Darby canine kidney epithelial cells (MDCK) and Vero cells (Vero) are indicated by open inverted triangles and open circles, respectively, and their curves are indicated by solid and dotted lines, respectively. The uptake of lysoPC by the various cells was normalized to cell number. The best fit curves were generated by NONLIN84 using mechanism 2.

tein-bound lysoPC remains at equilibrium; in other words, the rate constants k_4 and k_5 must be greater than k_1 and k_2 in mechanism 3.)

The kinetics of lysoPC association and metabolism by Vero cells in the presence of 0.5% FBS were described quite well by mechanism 3 (Figure 7, circles) and yielded the following rate constants: $k_4 = 0.8 \pm 0.4$ min^{-1}, $k_5 = 0.10 \pm 0.05$ M^{-1} min^{-1}, and $k_6 = (1 \pm 0.6) \times 10^{-7}$ min^{-1}. Futhermore, the dependence of lysoPC uptake as a function of the concentration of FBS, from 0 to 10%, was accurately described by mechanism 3 (Figure 7, curves). From these results, we can therefore conclude the following: mechanism 3 provides an accurate model of distribution, partitioning, and metabolism of exogenous lysoPC with Vero cells in the presence of serum proteins; the distribution of free lysoPC to serum protein-bound lysoPC remains at equilibrium in the presence of Vero cells; the serum protein (BSA) acts only as a sink for lysoPC, and the decrease in rates of cellular uptake of lysoPC with increasing FBS concentration is simply due to a decrease in the concentration of free lysoPC in the culture medium. Finally, the observation that the BSA-bound state of the lysoPC acts almost solely as an exogenous sink and does not significantly contribute to lysoPC uptake places an upper limit on k_6 of 10^{-5} min^{-1}. At this rate k_6 corresponds to cellular uptake at a rate of 15 nL·min^{-1} per 10^6 cells, a rate very consistent with known rates of fluid-phase pinocytosis (Besterman et al., 1981).

Kinetics of Association and Metabolism of Exogenously-Derived lysoPC Are Cell-Type Dependent. To determine whether the behavior of Vero cells might be expected to be representative of cultured mammalian cells in general, a preliminary survey of a variety of arbitrarily chosen cell types was performed. Surprisingly, there appears to be an enormous variability in the rate of uptake of exogenously-derived lysoPC with different cell types (Figure 8). These differences are intrinsic to the cell type since all the experiments were performed under identical experimental conditions. Furthermore, the differences in rates were not due to cell-specific conditioning of the media. As observed for Vero and neuronal cells, the rate of lysoPC association for each cell type was insensitive to whether the cell was incubated under standard conditions or bathed in the conditioned medium of the other cell (data not shown).

Discussion

The use of exogenous radiolabeled lysoPC as a precursor pool for the synthesis of a labeled pool of cell membrane PC has largely gone unexplored. Savard and Choy (1982) reported that perfused hamster hearts converted exogenous 1-palmitoyl-lysoPC to cell membrane associated PC by uptake and reacylation at a rate approximately equal to 35 nmol/min (g of heart protein)$^{-1}$. Conversion of the data reported here for Vero cells to similar units yielded 31 nmol/min (g of cell protein)$^{-1}$. In light of the cell-type-dependent variation in the rate of lysoPC association and cellular metabolism (Figure 8), it is almost surprising how similar the rates for Vero cells in culture and perfused hamster heart are. It is at least curious, however, that lysoPC is cleared very slowly by brain-derived cell types as a class. Whether this in some way is an important

reflection of central nervous system membrane composition and function is not known.

Thus far, our work has been limited to studies with 1-palmitoyl-lysoPC. We do not know whether the kinetics of association and metabolism of exogenously-derived lysoPC with cultured cells are dependent on the fatty acid component. In this regard, mammalian cells are known to contain lysophospholipases (van den Bosch, 1982), and thus, it would not be unreasonable to expect to observe the formation of free [^{14}C]palmitate from exogenously-provided [^{14}C]palmitate lysoPC. In Vero cells we always observed a small pool of free fatty acid formed in a time-dependent manner. This pool never exceeded 1% of the total cell-associated radiolabel, nor did this pool accumulate in the media. In contrast, in Vero cells heat-inactivated at 60 °C for 5 min, free [^{14}C]palmitate comprised 27% of the cell-associated radiolabel. Thus, in Vero cells there may be two pathways competing for lysoPC as substrate. Under normal basal conditions, the acyltransferase appears favored, resulting in almost complete conversion to PC with only minor conversion to free fatty acid. However, when the acyltransferase is inactivated, as by heating, the activity of the lysophospholipase predominates, resulting in the formation of free fatty acid. The balance of these two metabolic pathways may be cell-type specific, as free fatty acids are a major metabolite in erythrocytes exposed to exogenous lysoPC under normal conditions (Tamura et al., 1985).

In model lipid vesicles the transbilayer movement (flip-flop) of phospholipids and lysophospholipids is usually very slow, with overall half-lives on the order of days (Tamura et al., 1985; Dawidowicz, 1987; Bergmann et al., 1984). In isolated biological membranes, in general, the transmembrane movement of phospholipids and lysophospholipids is faster than in pure lipid vesicles, with overall half-lives on the order of minutes to hours (Dawidowicz, 1987). Unfortunately, however, outside of erythrocytes, little if any work has been performed to determine the rate of transmembrane diffusion of phospholipids and lysophospholipids. In this regard, the contribution of flip-flop to the kinetics of the metabolism of lysoPC by Vero cells is unknown. At present, our data do not distinguish between lysoPC located in the inner and the outer membrane leaflets. Several laboratories have demonstrated that BSA can be used to measure the inner to outer membrane leaflet distribution of lysoPC (Tamura et al., 1985; Bergmann et al., 1984; Mohandras et al., 1982). We have begun these types of studies.

Lipid-phase transitions in mammalian cell membranes occur over a range of temperatures, usually centered around 20–25 °C (Rule et al., 1980; Ryan & Simoni, 1980; Burns & Dudley, 1982). Despite the multiple lipid states that are thought to simultaneously coexist in a mammalian cell traversing the phase-transition temperature region, mammalian cell functions involving the membrane sometimes demonstrate acute sensitivity to alterations in temperature as reflected by a single, sharp break in Arrhenius plots in the range of 20–25 °C (Melchior & Stein, 1976; Rule et al., 1980; Ryan & Simoni, 1980; Burns & Dudley, 1982). As the Arrhenius plot of Figure 3 shows, the association and metabolism of lysoPC by Vero cells exhibit a 10-fold change in slope around 21 °C. Within the limits of the model described by mechanism 2, dissection of the temperature dependence revealed that k_2 was uniformly temperature sensitive over the entire temperature range (15–37 °C), and k_1 showed a break between 23 and 37 °C which did not correspond to a break in the overall process. However, k_3 was approximately 5-fold more sensitive to temperature below 23 °C than above 23 °C (Figure 4A and Table I), as was the overall half-life. Therefore, the temperature dependence of k_3 alone is largely responsible for the macroscopic temperature dependence exhibited by the overall process of cell association and metabolism of exogenously-derived lysoPC.

Why is k_3 so acutely temperature sensitive? One possibility is that the mechanism of enzyme catalysis is acutely sensitive to the physical state of the membrane lipids. Another possibility is that k_3 includes another step, endocytosis of membrane vesicles. Conventional wisdom dictates that the reacylation enzymes are located in the endoplasmic reticulum (Mohandras et al., 1982). Thus, how do the enzymes access lysoPC in the plasma membrane? This possible complication raises the possibility that endocytosis of plasma membrane to or through the ER is required. A role for endocytosis would be consistent with the acute temperature sensitivity of k_3, and previous work has demonstrated that endocytosis can be acutely temperature sensitive (Lands, 1960; Weigel & Oka, 1981; Shirazi et al., 1982). Therefore, although we have represented the rate constants as individual chemical or physical steps, these rate constants may represent the flux through several steps. For example, k_3 may include transmembrane movement of lysoPC and endocytosis of plasma membrane vesicles. Our data is not yet detailed enough to include and quantify transmembrane movement and membrane internalization into our model of lysoPC metabolism.

The cellular association and metabolism of lysoPC by Vero cells was measured and modeled under conditions of 0–10% FBS. In the presence of 0–0.5% FBS, a simple, two-step model (mechanism 2, discussed above) consisting of a reversible partitioning of exogenous lysoPC into the cell membrane followed by enzymatic reacylation to PC was found to adequately describe the observed kinetics. However, to accurately describe the kinetics observed in the presence of 2.5 and 10% FBS, mechanism 2 had to be expanded so as to allow for the existence of both free lysoPC and lysoPC bound to serum protein (mechanism 3). By combining the kinetic constants determined under conditions of low exogenous protein (0.5% FBS or less), with the binding constant for lysoPC–serum protein interaction, as determined by gel electrophoresis, we were able to accommodate lysoPC binding to serum protein in a multistep model (mechanism 3) and accurately predict the rates of uptake of exogenously-derived lysoPC with cultured cells in the presence of serum concentrations of 0–10%.

Acknowledgments

We thank Dr. Paul Morgan for introducing us to NONLIN84, Dr. Harry LeVine III for suggesting the heat inactivation approach, Dr. David Bruckenstein for providing some of the rat brain-derived cell types, and Esther Joo Lee, Peter Leitner, Irene Zajac, Dr. Ana Cortizo, and Jim Nichols for excellent technical assistance. We also thank Drs. Paul Morgan and Jeff Wiseman for a critical reading of the manuscript.

References

Avruch, J., & Wallach, D. F. H. (1971) *Biochim. Biophys. Acta 233*, 334–347.

Bergmann, W. L., Dressler, V., Haest, C. W. M., & Deuticke, B. (1984) *Biochim. Biophys. Acta 772*, 328–336.

Besterman, J. M., Airhart, J. A., Woodworth, R. C., & Low, R. B. (1981) *J. Cell Biol. 91*, 716–727.

Burgess, S. K., Jacobs, S., Cuatrecasas, P., & Sahyoun, N. (1987) *J. Biol. Chem. 262*, 1618–1622.

Burgess, S. K., Sahyoun, N., Blanchard, S. G., LeVine, H., III, Chang, K. J., & Cuatrecasas, P. (1986) *J. Cell Biol. 102*, 312–319.

Burgess, S. K., Trimmer, P. A., & McCarthy, K. (1985) *Brain Res. 335*, 11-19.
Burns, C. P., & Dudley, D. T. (1982) *Biochem. Pharmacol. 31*, 2116-2119.
Chapman, D. (1975) *Biomembranes 7*, 1-9.
Dawidowicz, E. A. (1987) *Annu. Rev. Biochem. 56*, 43-61.
Golan, D. E., Brown, C. S., Cianci, C. M. L., Furlong, S. T., & Caulfield, J. P. (1986) *J. Cell Biol. 103*, 819-828.
Hartley, H. O. (1961) *Technometrics 3*, 269-280.
Hoffman, R. D., Kligerman, M., Sundt, T. M., Anderson, N. D., & Shin, H. S. (1982) *Proc. Natl. Acad. Sci. U.S.A. 79*, 3285-3289.
Kuby, S. A., Node, L., & Lardy, H. A. (1954) *J. Biol. Chem. 209*, 191.
Lands, W. E. M. (1960) *J. Biol. Chem. 235*, 2233-2237.
Melchior, D. L., & Stein, J. M. (1976) *Annu. Rev. Biophys. Bioeng. 5*, 205-237.
Mohandras, N., Wyatt, J., Mel, St. F., Rossi, M. E., & Shohet, St. B. (1982) *J. Biol. Chem. 257*, 6537-6543.
Quinn, M. T., Parthasarathy, S., & Steinberg, D. (1988) *Proc. Natl. Acad. Sci. U.S.A. 85*, 2805-2809.
Rule, G. S., Law, P., Kruuv, J., & Lepock, J. R. (1980) *J. Cell Physiol. 103*, 407-416.
Ryan, J., & Simoni, R. D. (1980) *Biochim. Biophys. Acta 598*, 606-615.
Savard, J. D., & Choy, P. C. (1982) *Biochim. Biophys. Acta 711*, 40-48.
Shirazi, M. F., Aronson, N. N., & Dean, R. T. (1982) *J. Cell Sci. 57*, 115-127.
Tamura, A., Tanaka, T., Yamana, T., Nasu, R., & Fujii, T. (1985) *J. Biochem. (Japan) 97*, 353-359.
van den Bosch, H. (1982) *Phospholipids* (Hawthorne, J. N., & Ansell, G. B., Eds.) Chapter 9, Elsevier Biomedical Press, Amsterdam.
Weigel, P. H., & Oka, J. A. (1981) *J. Biol. Chem. 256*, 2615-2617.

Structural Elements of Human Parathyroid Hormone and Their Possible Relation to Biological Activities†

W. Neugebauer, W. K. Surewicz,* H. L. Gordon, R. L. Somorjai, W. Sung, and G. E. Willick*
Protein Structure and Function Section, Institute for Biological Sciences, National Research Council of Canada, Ottawa, Canada K1A OR6

Received July 29, 1991; Revised Manuscript Received October 28, 1991

ABSTRACT: Human parathyroid hormone (hPTH) and several deletion analogues were examined for the presence of secondary structure using circular dichroism spectroscopy. The spectra of hPTH and the deletion analogues 8-84, 34-53, 53-84, 1-34, 13-34, 1-19, and 20-34, in neutral, aqueous buffer, gave no evidence for extensive secondary structure. An α-helical-like spectral contribution was found to arise from a region within peptide 13-34. This spectral contribution was speculated to arise from partial stability of a helix consisting of residues 17-29. Molecular dynamics simulations of peptide 1-34 suggested that this peptide tends to fold with a bend defined by residues 10-14, with the amino-terminal and carboxyl-terminal residues tending to be in more extended forms and the other residues in helical-like conformations. The addition of trifluoroethanol promoted the formation of α-helix, mainly in the 1-34 region. The putative helix comprised of residues 17-29 was stabilized by the addition of 10-20% TFE, while a second putative helix proximal to the amino terminus, and comprised of residues 3-11, was stabilized by slightly higher concentrations of TFE. An amphiphilic sequence was identified within the 20-34 fragment. The development of α-helix on binding this fragment, and other analogues containing this sequence, to palmitoyloleoylphosphatidylserine vesicles provided experimental evidence for the potential role of this amphiphilic sequence in binding to membranes or to a membrane receptor. The relationships between these α-helical regions in 1-34, either potentiated by trifluoroethanol or lipid vesicles, are discussed in terms of different receptor-binding regions within hPTH.

Parathyroid hormone (PTH)[1] plays a major role in regulating circulating calcium levels through effects on the kidney and on resorption and deposition of calcium in bone. The full-sized hormone is 84 residues long and has recently become available in quantities as a result of expression of the gene in *Escherichia coli* (Hogset et al., 1990; Sung et al., 1991). However, almost all of the reported in vitro activities require only sequences within the 1-34 segment, and consequently this is the region about which most studies have centered.

The biological activity of hPTH has been monitored extensively by measuring adenylate cyclase activation and by radioreceptor assays using kidney or bone tissue or cultured cells (Jüppner, 1989). In these two assays, PTH and the 1-34 fragments are equally active. For stimulation of adenylate cyclase, almost all of the 1-34 sequence is required, including the NH_2-terminal serine or alanine. In contrast, a recently reported mitogenic effect (Schlüter et al., 1989) and a stimulation of protein kinase C activity (Jouishomme et al., 1992)

† This is National Research Council of Canada Publication No. NRC 31986.
* Authors to whom correspondence should be addressed.

[1] Abbreviations: PTH, human parathyroid hormone; hPTH, human PTH; CD, circular dichroism; TFE, trifluoroethanol; POPS, 1-palmitoyl-2-oleoylphosphatidylserine.

0006-2960/92/0431-2056$03.00/0 Published 1992 by the American Chemical Society